PHYSICAL REVIEW B VOLUME 59, NUMBER 24 15 JUNE 1999-II

Calculation of the wave functions for semi-infinite crystals with linear methods of band theory

E. E. Krasovskii and W. Schattke
Institut für Theoretische Physik, Christian-Albrechts-Universität, Leibnizstrasse 15, D-24118 Kiel, Germany
(Received 15 October 1998; revised manuscript received 16 February 1999)

We present a variational method to solve the Schrödinger equation for a semi-infinite crystal. The complex band structure is generated by the inverse extended linear augmented plane wave $\mathbf{k}\cdot\mathbf{p}$ method. The trial function is continuous and smooth over the whole space and it satisfies by construction the equation $(\hat{H}-E)\Phi=0$ both in the crystal and in the vacuum half-spaces. In the surface region the equation $\delta\|(\hat{H}-E)\Phi\|=0$ is solved. The formalism is applicable to potentials of general shape in the surface region. The procedure is applied to calculations of low energy electron diffraction spectra for the (111) surfaces of the fcc metals Cu, Ag, Ni, Pd, and Al. [S0163-1829(99)50124-0]

I. INTRODUCTION

A semi-infinite crystal is a three-dimensional (3D) system with a 2D periodicity that is composed of bulk and vacuum half-spaces separated by a slab inside that the crystal potential changes from its bulk distribution to a constant value in the vacuum. The present day methods to solve the Schrödinger equation for a semi-infinite solid can be divided into two groups with regard to the role of the imaginary part of the potential (optical potential) in the computational formalism. The optical potential describes the inelastic scattering of the electrons in the crystal and it causes the wave function to decay, which makes it possible to restrict the computations to a finite number of monolayers. That feature is exploited in the multiple-scattering approach[1] and in the purely direct-space methods,[2] which yield efficient computational schemes for rapidly decaying wave functions, however, the computational effort grows by decreasing the value of the optical potential. On the contrary, in the Bloch waves approach[3,4] the computational effort does not depend upon the value of the optical potential. The latter technique is applicable also to the case of the zero optical potential; in that case inside the crystal far from surface the solution is a linear combination of the wave functions that satisfy the bulk Schrödinger equation, and the problem of very low energy electron diffraction[5] (VLEED) is solved within the traditional no-absorption quantum-mechanical picture.

In the present paper we consider the application of the Bloch-wave based techniques to the calculation of the LEED states. In such methods the trial function is constructed separately in each of the three regions and the wave function is usually obtained by matching the trial functions at the boundary surfaces. With a finite number of bulk partial solutions (propagating and evanescent Bloch waves, Ψ_n) the functions cannot be matched exactly, and the approximate wave function has a discontinuity in slope (in some schemes also in value) at the matching plane. There is no physical criterion for deciding whether the mismatch is sufficiently small. The very definition of mismatch is not unambiguous; consequently, there exist a number of matching approaches that minimize different quantities. Several matching schemes have been studied in Ref. 6, and it has been shown that, in general, the calculated observables (reflected intensities in the case of LEED) are not stable to the residual mismatch. Furthermore, one cannot rely upon the convergence of the procedure because only a limited number of evanescent Bloch waves have satisfactory quality. (The accuracy of the wave function deteriorates rapidly with the growth of the imaginary part of the Bloch vector irrespective of the computational method.[6])

Within the Bloch waves approach two methods have been developed to treat the wave function in the surface region: Appelbaum and Hamann[7] solved the Schrödinger equation by a step-by-step integration, and Hummel and Bross[8] sought the function as a linear combination of partial solutions that form a set for all possible boundary conditions of the Dirichlet type. In both cases the problem splits into two parts: integrating the Schrödinger equation and determining the boundary conditions for the specific solution. The latter task involves matching and it introduces an error irrespective of the quality of the integration.

Practical treatment of the semi-infinite crystal problem depends upon the answer to the question: what is the best possible wave function for a given set of bulk partial solutions? We propose a physically transparent energy criterion: for a given energy E and a given set of functions Ψ_n we construct a smoothly continuous function Φ that minimizes the energy deviation $\|(\hat{H}-E)\Phi\|$ under constraints dictated by the physical nature of the problem. For the methods in which the partial solutions are variational wave functions this is a natural criterion: when the quality of the trial function becomes comparable to the quality of the individual partial solutions the inclusion of more evanescent states would not improve the results.

In Sec. II, we present the formalism of the method and in Sec. III we apply the method to the analysis of the LEED spectra of (111) surfaces of fcc metals.

II. FORMALISM

The representation of the wave function for the case of a propagating electron (LEED regime) is shown in Fig. 1. In the bulk region, $z<0$, the crystal potential does not change from layer to layer, in the vacuum region, $z>L$, it is con-

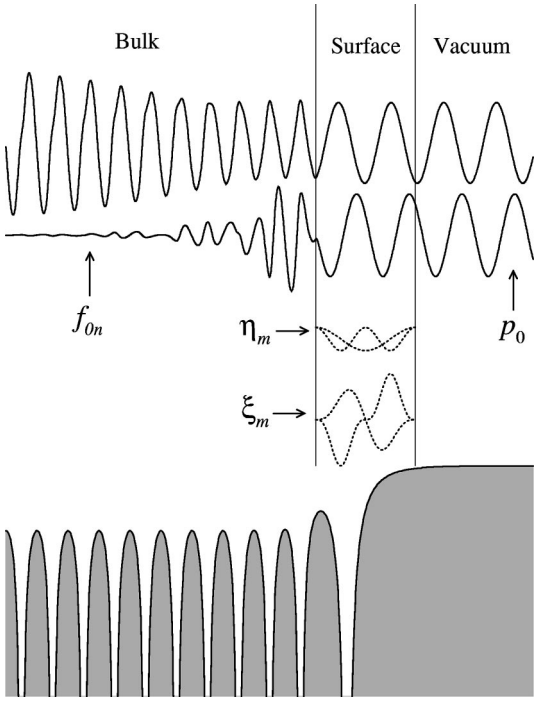

FIG. 1. Representation of the wave functions in the variational method. The set of Bloch functions analytically extended to the vacuum (X_n, solid lines) is supplemented with a set of periodic functions ($\xi_m(z)\exp[i\mathbf{K}_s\boldsymbol{\rho}]$ and $\eta_m(z)\exp[i\mathbf{K}_s\boldsymbol{\rho}]$, see Eqs. (6) and (7); dotted lines). $G_s=0$ components are shown. The functions X_n are calculated for the (111) surface of Al, for $E-E_F=14$ eV.

stant, and in the surface region, $0<z<L$, the potential has a 2D periodicity. The LEED state $\Phi(\boldsymbol{\rho},z)$ is defined by its energy E and the surface projection of the Bloch vector $\mathbf{k}_\parallel$. In the bulk the LEED state is a linear combination of propagating and evanescent Bloch states, Ψ_n, which for given E and $\mathbf{k}_\parallel$ are generated by the inverse extended linear augmented plane wave (ELAPW) $\mathbf{k}\cdot\mathbf{p}$ method,[6]

$$\Psi_n(\boldsymbol{\rho},z)=\sum_{s=0}^{N_F-1} f_{sn}(z)\exp[i\mathbf{K}_s\boldsymbol{\rho}], \quad z<0. \tag{1}$$

Here $\mathbf{K}_s=\mathbf{k}_\parallel+\mathbf{G}_s$, $\mathbf{G}_s$ being the surface reciprocal lattice vectors; $\mathbf{G}_0=0$. We now analytically continue the functions Ψ_n to the half-space $z>0$. The functions $f_{sn}(z)$ with $G_s\neq 0$ are extended by attaching a linear combination of two tails: a ''physical'' tail, which has a correct asymptotics at $z\to+\infty$, and an auxiliary tail, which decays rapidly with the distance from the surface. The ''physical'' tail

$$p_s(\boldsymbol{\rho},z)=\exp[i\mathbf{K}_s\boldsymbol{\rho}+ik_sz], \quad K_s^2+k_s^2=E, \tag{2}$$

may be a propagating wave $\mathrm{Im}\,k_s=0$ or an evanescent wave $\mathrm{Im}\,k_s>0$, depending on E and K_s^2. The auxiliary tail

$$a_s(\boldsymbol{\rho},z)=\exp[i\mathbf{K}_s\boldsymbol{\rho}+iq_sz], \quad K_s^2+q_s^2=E_0, \tag{3}$$

is always an evanescent plane wave $\mathrm{Im}\,q_s>0$. The auxiliary energy E_0 is taken considerably lower than E, so that the auxiliary tails decay fast and are negligible for $z>L$. For $G_s=0$ the physical part $p_0(z)$ is always propagating: it is a linear combination of the incoming and the outgoing (central beam) plane wave. Thus any linear combination of the extended functions (which we shall refer to as X_n, solid lines in Fig. 1) satisfies the Schrödinger equation both in the vacuum half-space and (with a certain accuracy) in the bulk. The error is confined to the surface region. To compensate for it we must add to a linear combination of X_n a set of functions U_s, which are nonzero only in the surface region,

$$U_s(\boldsymbol{\rho},z)=u_s(z)\exp[i\mathbf{K}_s\boldsymbol{\rho}], \quad 0<z<L. \tag{4}$$

Functions $u_s(z)$ go to zero with zero derivative at $z=0$ and $z=L$. The functions U_s and the coefficients of the functions X_n are determined by minimizing the value $\|(\hat{H}-E)\Phi\|$, which is an integral over the surface region,

$$\|(\hat{H}-E)\Phi\|=\int_0^L\int_{\Omega_s}|(\hat{H}-E)\Phi(\boldsymbol{r})|^2\,d\boldsymbol{\rho}\,dz. \tag{5}$$

The problem is reduced to a linear algebra problem by expanding the functions $u_s(z)$ in terms of odd $\xi_m(z)$ and even $\eta_m(z)$ linear combinations of standing plane waves (dotted lines in Fig. 1),

$$\xi_m(z)=\sin\frac{2\pi mz}{L}-m\sin\frac{2\pi z}{L}, \tag{6}$$

$$\eta_m(z)=\cos\frac{2\pi mz}{L}-1, \tag{7}$$

$$\Phi(\mathbf{r})=\sum_n a_nX_n(\boldsymbol{r})+\sum_{sm}[p_{sm}\xi_m(z)+q_{sm}\eta_m(z)]e^{i\mathbf{K}_s\boldsymbol{\rho}}. \tag{8}$$

$\{a_n\}$ and $\{p_{sm},q_{sm}\}$ comprise the set of variational coefficients and the asymptotics of the wave function at $z\to+\infty$ or $-\infty$ (reflected or transmitted current) is determined by the set $\{a_n\}$. An important feature of this formalism is that although the potential in the surface region is not periodic in the z direction the wave function is represented by a number of plane waves. Their wave vectors do not form a lattice in reciprocal space, and some of them are complex; however, the plane wave ansatz makes it straightforward to extend the formalism to the case of a singular potential in the surface region (adsorbate atoms or a reconstructed surface). In such cases the plane waves can be augmented in the vicinity of the nuclei using one of the standard APW techniques of band theory. Similarly to the variational matching technique[6] the minimization of $\|(\hat{H}-E)\Phi\|$ under the constraint that the incident current is equal to unity (LEED regime) leads to a system of linear equations. In the case of bounded states (no incident waves) it leads to an eigenvalue problem.

III. TARGET CURRENT SPECTRA

To calculate the VLEED spectra of the (111) surfaces of fcc metals we have implemented the above formalism for the simplified case of a step potential barrier. Here the surface region is reduced to zero, the functions U_s are dropped, and the integration in Eq. (5) extends to $L=\infty$. In Fig. 2 we present the normal incidence target current spectra (TCS) of Cu and Ag, i.e., the portion of the incident current transmitted to the solid versus the energy of the incident electron beam. The results for Ni and Pd are presented in Fig. 3.

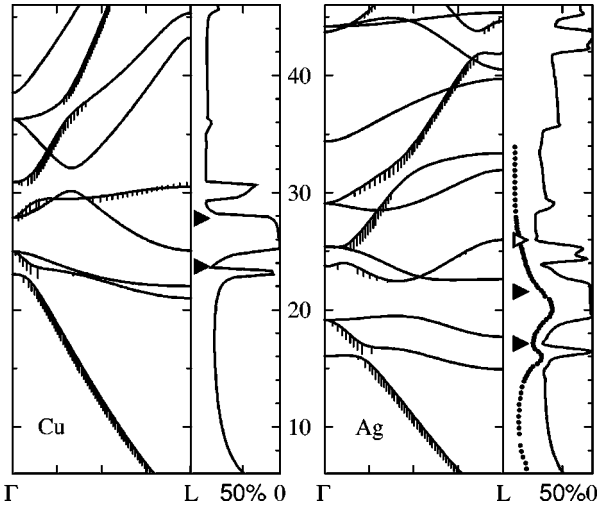

FIG. 2. In the right panels: the TCS spectra of the (111) surfaces of Cu and Ag. The TCS obtained from the VLEED measurements of Ref. 11 is shown by a dotted line (the curve is arbitrarily shifted in energy). The energy positions of the TCS minima found experimentally in Ref. 9 are shown by triangles; two pronounced minima are shown by filled triangles and a weak structure is shown by an empty triangle. In the left panels: the real band structure $E(k_z)$ in the ΓL direction calculated with the usual ELAPW method. Energies are in eV relative to the Fermi level. The Bloch waves responsible for the transmisson of the current are marked by ''error bars''; the length of the whisker is proportional to the current carried by the wave. The upper end of the whisker shows the band structure $k_z(E)$ obtained with the inverse ELAPW $\mathbf{k}\cdot\mathbf{p}$ method. The deviation of the $k_z(E)$ points from the $E(k_z)$ curves shows the error of the $\mathbf{k}\cdot\mathbf{p}$ method.

The experimental spectra can be easily interpreted in terms of the real band structure: the main minima (at 26 eV for Cu and 21 eV for Ag) are due to local forbidden gaps formed by the (222) Bragg reflection.[9] Also the sharp experimental minima[9] at 23 eV in Cu and 16 eV in Ag are caused by the splitting of the real branches of the band structure. However, owing to the changing conducting properties of the current carrying Bloch states the gaps in the TCS curves are much wider than the forbidden energy gaps in the $\mathbf{k}_\parallel$-projected band structure (a vivid example is the main TCS minimum of Cu). Our results for Cu and Ag agree well with layer KKR (Ref. 1) calculations of Refs. 10 and 11, respectively. Our TCS spectrum of Cu agrees well with the measurements of Refs. 9, 10, and 12; earlier measurements[13] show an additional structure at $E-E_{\rm vac}=12.5$ eV, which we do not observe.

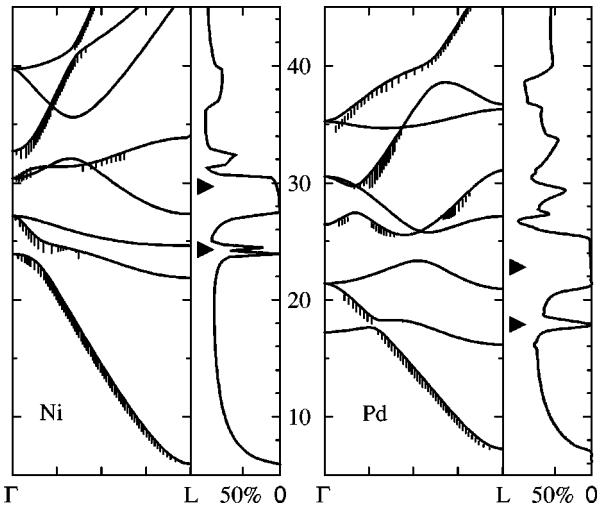

FIG. 3. Solid lines in the right panels show the TCS spectra of the (111) surfaces of Ni and Pd. The experimental TCS minima (Ref. 9) are shown by triangles. In the left panels: the real band structure $E(k_z)$ in the ΓL direction. See also the caption of Fig. 2.

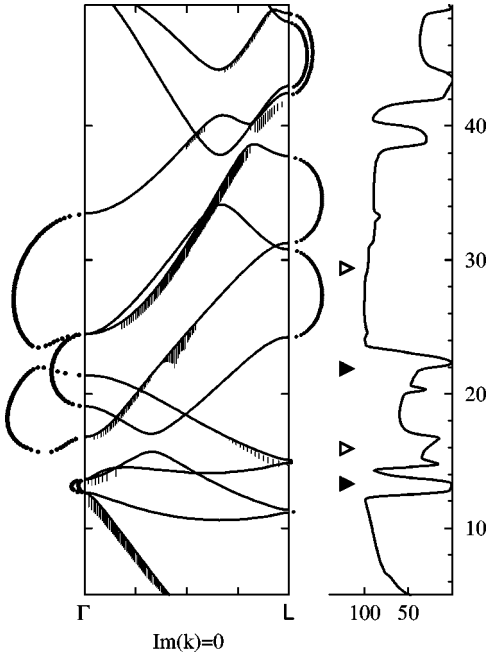

FIG. 4. Complex band structure and the target current spectrum of the (111) surface of aluminum. The experimental TCS minima (Ref. 9) are shown by triangles. Real lines of the complex band structure $E(\mathrm{Im}\,k_z)$ for $\mathrm{Re}\,k_z$ at Γ and at L are shown by dots to the right and to the left of the real band-structure panel, respectively. See also the caption of Fig. 2.

Figure 4 shows the target current spectrum of Al. As in the above cases the structures at 13 and 16 eV have a ''real band-structure origin.'' Contrastingly, the minimum at $\sim$22 eV cannot be ascribed to any peculiarities of the real band structure. The character of the current carrying band changes steadily, and the special point at 22.3 eV is caused by a strong effect of a branch of the complex band structure that contributes to the LEED wave function (see the left panel of Fig. 4). The minimum in the TCS curve occurs close to the turning point of the line $\mathrm{Re}\,k_z=0$ that extends from $E-E_F=18.8$ to 24.4 eV. There the character of the evanescent state changes rapidly, $dE/d\,\mathrm{Im}(k_z)=\infty$, causing a void at $E-E_F=22.3$ eV, $k_z=0.4|\Gamma L|$.

Figure 5 shows calculated TCS curves of the Cu (111) surface for several $\mathbf{k}_\parallel$ vectors in the LW direction of the fcc Brillouin zone (BZ). The sharp low energy structure is highly dispersive: it shifts downward (by $\sim$0.2 eV at $k_\parallel=0.08|\mathrm{LW}|$) and completely disappears at $k_\parallel=0.16|\mathrm{LW}|$. This behavior has been experimentally observed by Jaklevic and Davis[9] and by Strocov *et al.*[12]

A disagreement between theory and experiment in the energy locations of the two characteristic TCS features (a sharp minimum followed by a broad Bragg minimum) reflects the

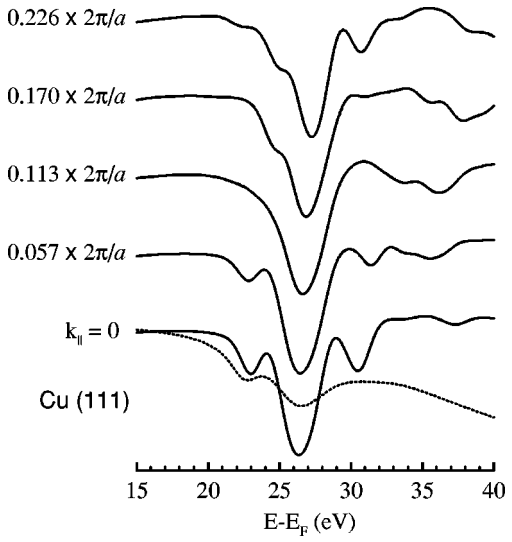

FIG. 5. Calculated TCS spectra of the (111) surface of Cu for several $\mathbf{k}_{\parallel}$ vectors parallel to the LW line of the 3D BZ. The curves are convoluted with a Gaussian of 1.5 eV full width at half maximum. The experimental normal-incidence TCS curve (Ref. 12) is shown by a dotted line (the curve is arbitrarily shifted in energy).

self-energy corrections to the band energies. Such discrepancies have turned out to be noticeable only for Cu and Ag; for both metals the experimental structures occur ~ 0.7 eV higher in energy than the theoretical ones (see Fig. 2). In Ni and Pd (see Fig. 3) the characteristic features occur at essentially the same energies as in Cu and Ag, respectively, but we see no energy shifts. We assume that the strong electron correlation in the highly localized *d* shells of the noble metals makes the one-electron model used in the present calculations less appropriate for Cu and Ag than for the other metals considered.

The developed method of the calculation of the electron states in a semi-infinite crystal is based on solving the Schrödinger equation in the surface region by means of a variational technique. Being a static method, it offers an interpretation of LEED spectra in terms of the complex band structure. For (111) surfaces of Ni, Cu, Pd, and Ag the experimentally observed TCS minima are explained by the features of the real band structure. In the TCS of Al a structure has been detected for which a special point in the evanescent part of the band structure is responsible. The energy locations of the characteristic TCS features are in good agreement with the experiment.

ACKNOWLEDGMENTS

We are indebted to Professor I. Bartoš and to Dr. V. Strocov for stimulating discussions. We are grateful to Dr. V. Strocov for making his measurements available to us prior to publication. One of the authors (E.E.K.) gratefully acknowledges support by a grant of the Alexander von Humboldt-Stiftung. This work was included in Project No. 05SB8FKA7 supported by the BMBF.

[1] J. B. Pendry, *Low Energy Electron Diffraction* (Academic Press, London, 1974); M. A. Van Hove and S. Y. Tong, *Surface Crystallography by LEED*, Springer Series in Chemical Physics Vol. 2 (Springer-Verlag, Berlin, 1979), and references therein.

[2] S. Lorenz, C. Solterbeck, W. Schattke, J. Burmeister, and W. Hackbusch, Phys. Rev. B **55**, 13 432 (1997), and references therein.

[3] D. S. Boudreaux and V. Heine, Surf. Sci. **8**, 426 (1967).

[4] J. B. Pendry, J. Phys. C **2**, 2273 (1969).

[5] V. N. Strocov, R. Claessen, G. Nicolay, S. Hüfner, A. Kimura, A. Harasawa, S. Shin, A. Kakizaki, P. O. Nilsson, H. I. Starnberg, and P. Blaha, Phys. Rev. Lett. **81**, 4943 (1998).

[6] E. E. Krasovskii and W. Schattke, Phys. Rev. B **56**, 12 874 (1997).

[7] J. A. Appelbaum and D. R. Hamann, Phys. Rev. B **6**, 2166 (1972).

[8] W. Hummel and H. Bross, Phys. Rev. B **58**, 1620 (1998).

[9] R. C. Jaklevic and L. C. Davis, Phys. Rev. B **26**, 5391 (1982).

[10] I. Bartoš, P. Jaroš, A. Barbieri, M. A. Van Hove, W. F. Chung, Q. Cai, and M. S. Altman, Surf. Rev. Lett. **2**, 477 (1995).

[11] I. Bartoš, M. A. Van Hove, W. F. Chung, Z. He, and M. S. Altman, Surf. Sci. **402-404**, 697 (1998).

[12] V. N. Strocov and H. I. Starnberg (unpublished).

[13] L. R. Bedell and H. E. Farnsworth, Surf. Sci. **41**, 165 (1973).